Supporting Information

Engineering the Orientation, Density and Flexibility of Single Domain Antibodies on Nanoparticles to Improve Cell Targeting.

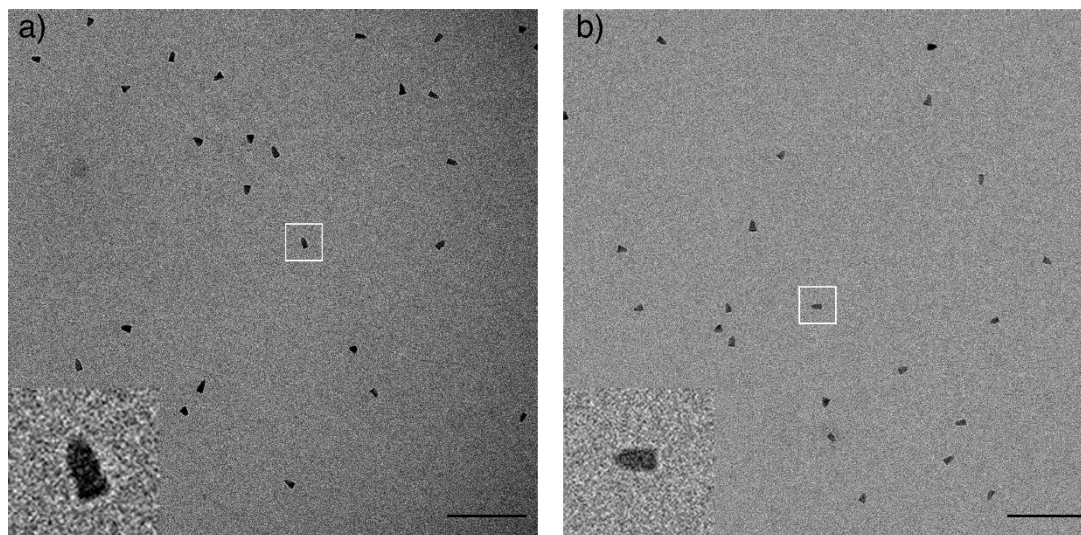Ken W. Yong, Daniel Yuen, Moore Z. Chen, Angus P. R. Johnston*

Drug Delivery, Disposition and Dynamics, Monash Institute of Pharmaceutical Sciences, Monash University, Parkville, Victoria 3052, Australia

ARC Centre of Excellence in Convergent Bio-Nano Science and Technology, Monash University, Parkville, Victoria 3052, Australia

*Email address of the corresponding author: angus.johnston@monash.edu

Characterization of sdAb conjugated Qdots.

Cryo-electron microscopy images (Figure S1) indicate that Qdots do not aggregate and retain their structure after immobilization of sdAbs onto Qdots even in cell media.

Figure S1. Cryo-electron microscopy images of a) azPhe13 oriented sdAb-Qdots and b) unmodified Qdots in Dulbecco's Modified Eagle Medium supplemented with 10% fetal bovine serum. Individual Qdots can be seen in a zoomed in image at bottom left corner of corresponding image. Individual sdAb-Qdots were found to be approximately 11.4 ± 1.0 nm x 7.2 ± 0.5 nm, n =10. Scale bar = 100 nm
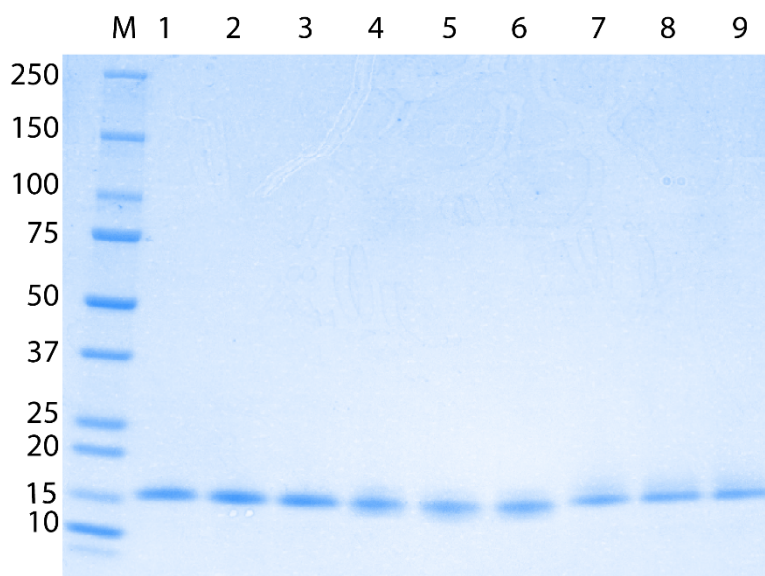
The zeta potential shown on Table S1 summarizes the shift in surface charge with presence of sdAb. A small decrease in zeta potential was observed with increasing linker PEG length.

Group	Zeta Potential (mV)
Unmodified Qdot	-19 ± 1
azPhe13	-10 ± 4
azPheCT	-7 ± 2
Random orientation	-11 ± 3
azPhe13 PEG$_4$	-14 ± 3
azPheCT PEG$_4$	-19 ± 3
Random orientation PEG$_4$	-16 ± 1
azPhe13 PEG$_{12}$	-29 ± 1
azPheCT PEG$_{12}$	-29 ± 3
Random orientation PEG$_{12}$	-31 ± 1

Table S1. ζ potential changes after immobilization of sdAb-biotin modification to Qdots. Data are presented as mean $\pm$ SD of n = 3 independent experiments.

Previous results indicated that the conjugated sdAb-Qdots demonstrated similar absorbance and fluorescence intensity to the unmodified Qdots in PBS and in cell media (DMEM).[1]
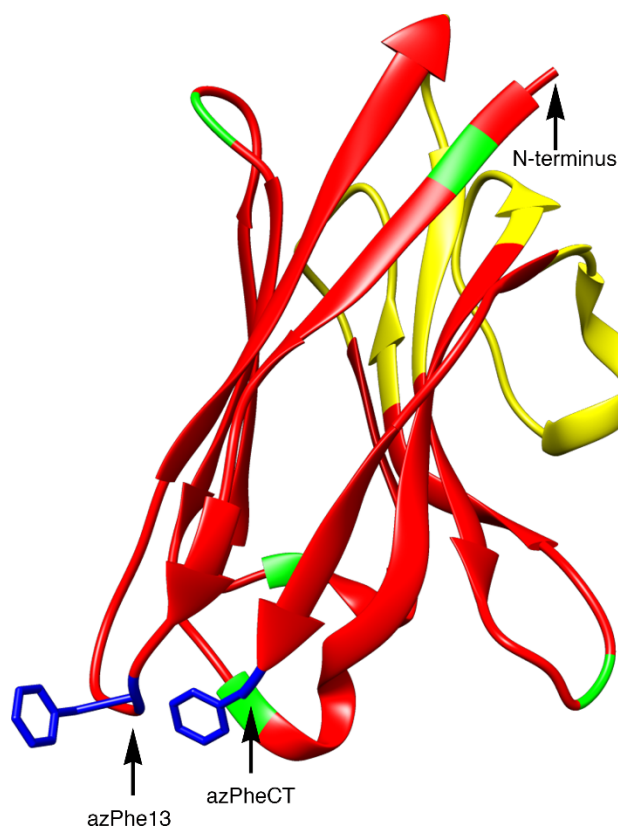
Data for determining the number of sdAb per Qdot was acquired from n = 3 independent experiments.[2,3] Figure S2 and Table S2 show example analysis from one of these independent experiments.
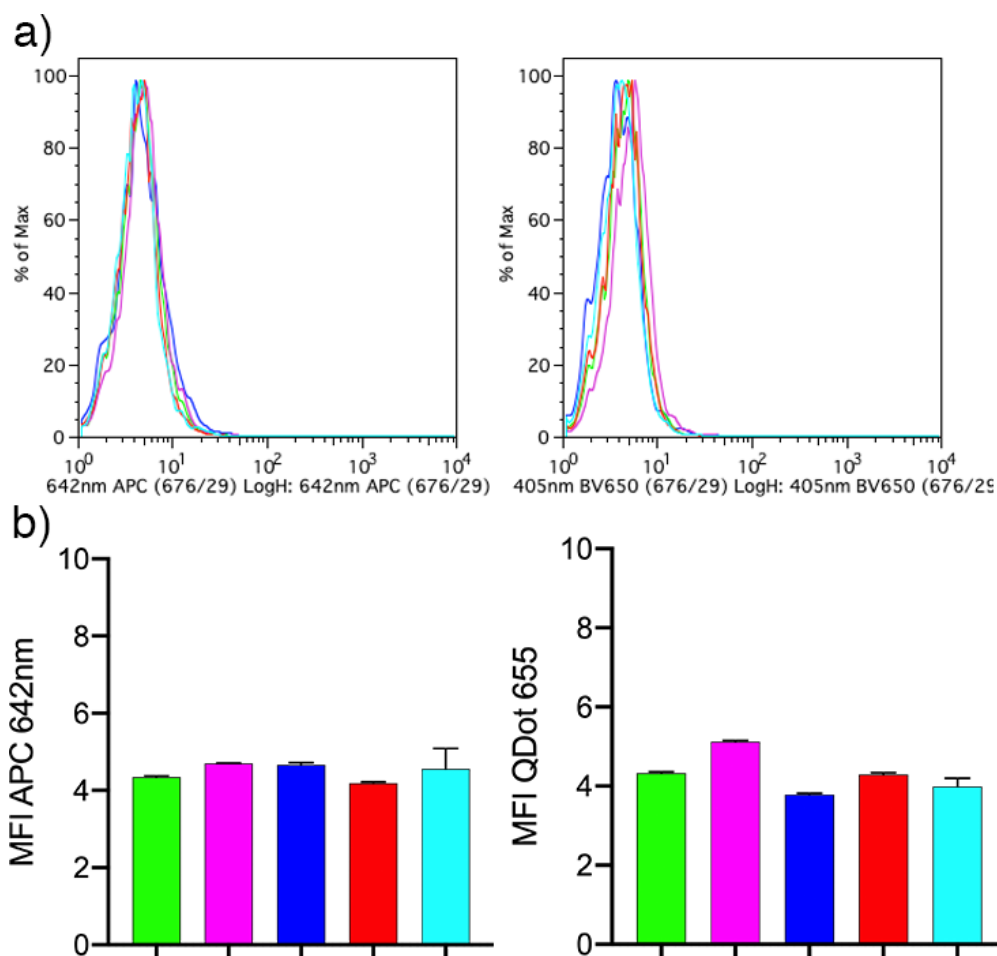

Figure S2. Non-reducing Coomassie stained SDS-PAGE of sdAb-biotin conjugate. A fixed amount of sdAb (138 pmole) was added to each lane (Lanes 1-3 (azPhe13), 4-6 (azPhe13 PEG$_4$) and 7-9 (azPhe13 PEG$_{12}$). Lanes 2, 5 and 8 were mixed with 2.3 pmole of Qdots and lanes 3, 6 and 9 were mixed with 1 pmole of Qdots. Unbound sdAbs can be seen as a single band at approximately 15 kDa. Fiji software was used to determine the density of each band (Table S2).

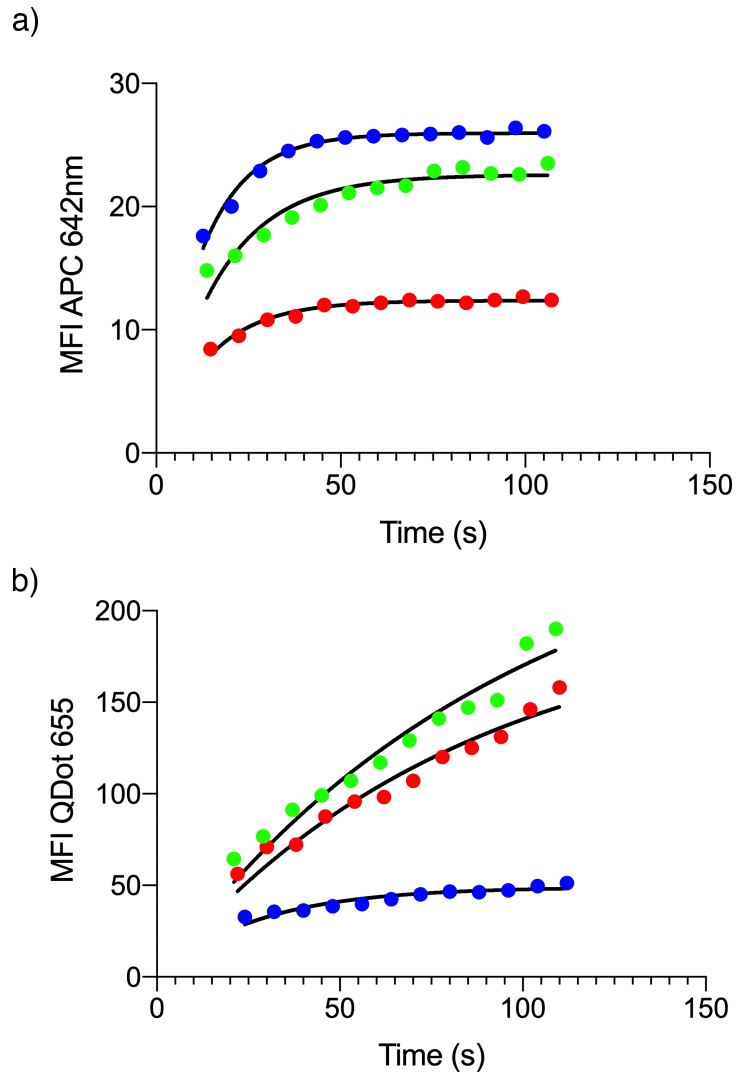| Lane	Sample	sdAb (pmole)	Qdot (pmole)	Density value	Difference	sdAb bound (%)	sdAb per Qdot
1	azPhe13	138	-	12910.3	-	NA	-
2	azPhe13	138	2.3	11833.1	1077.2	8.3	5
3	azPhe13	138	1.0	11112.3	1798.0	13.9	19
4	azPhe13 PEG$_4$	138	-	12102.1	-	NA	-
5	azPhe13 PEG$_4$	138	2.3	10699.8	1402.3	11.6	7
6	azPhe13 PEG$_4$	138	1.0	9889.9	2212.2	18.3	25
7	azPhe13 PEG$_{12}$	138	-	10008.9	-	NA	-
8	azPhe13 PEG$_{12}$	138	2.3	8754.6	1254.3	12.5	8
9	azPhe13 PEG$_{12}$	138	1.0	8590.0	1418.9	14.2	20

Table S2. The free sdAb band density analyzed from Figure S2 was used to calculate the percentage of sdAb bound to Qdots and subsequently the number of sdAb bound per Qdot.
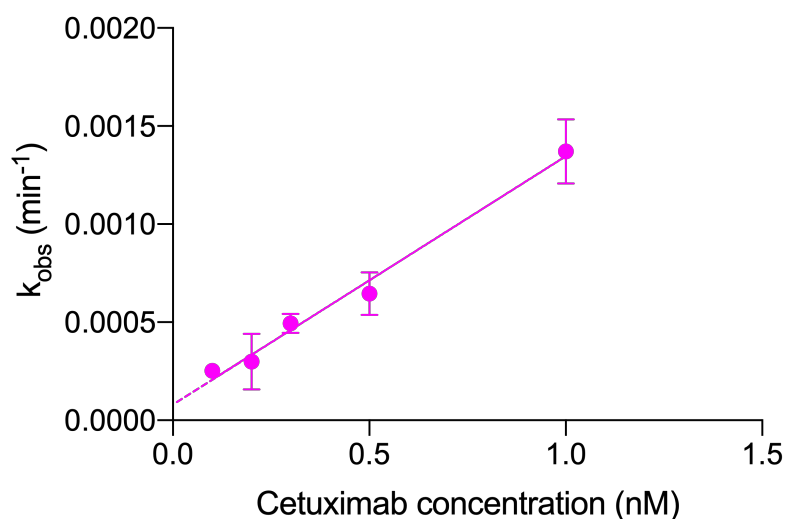
Figure S3. 3D representation of anti-EGFR sdAb. The binding site of sdAb is highlighted in yellow and azPhe incorporation (blue) replacing original glutamine-13 amino acid (azPhe13) or incorporation at C-terminus (azPheCT). Lysine residues are highlighted in green to show possible orientation of sdAb when NHS conjugation was used.
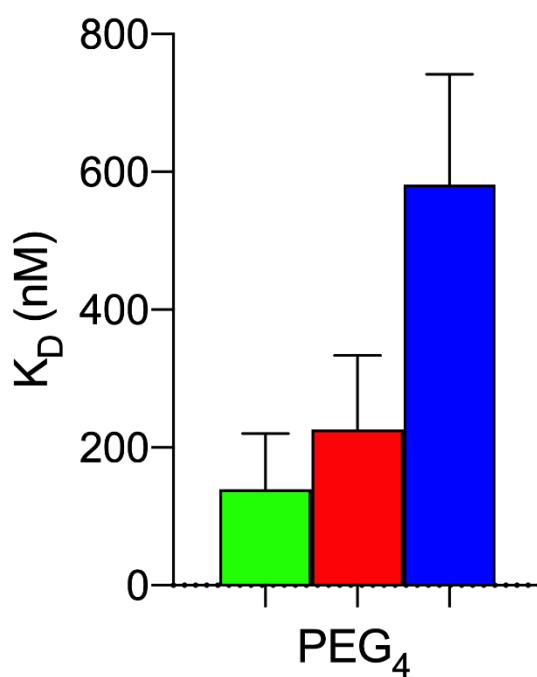
Figure S4. Mean fluorescence intensity of EGRF- 3T3 cells incubated with azPhe13 PEG$_4$ Qdots on a) raw flow cytometry histogram and b) analyzed histograms of 3T3-incubated cells. As a control, cetuximab (labeled with Cy5) was used alongside azPhe13 PEG$_4$ Qdots. Additionally, a higher concentration of azPhe13 PEG$_4$ Qdots (1.5 nM) was added to cells. Green – 1 nM azPhe13 PEG$_4$ Qdots, magenta – 1.5 nM azPhe13 PEG$_4$ Qdots, blue – cetuximab, red – unmodified Qdots, turquoise – untreated cells.
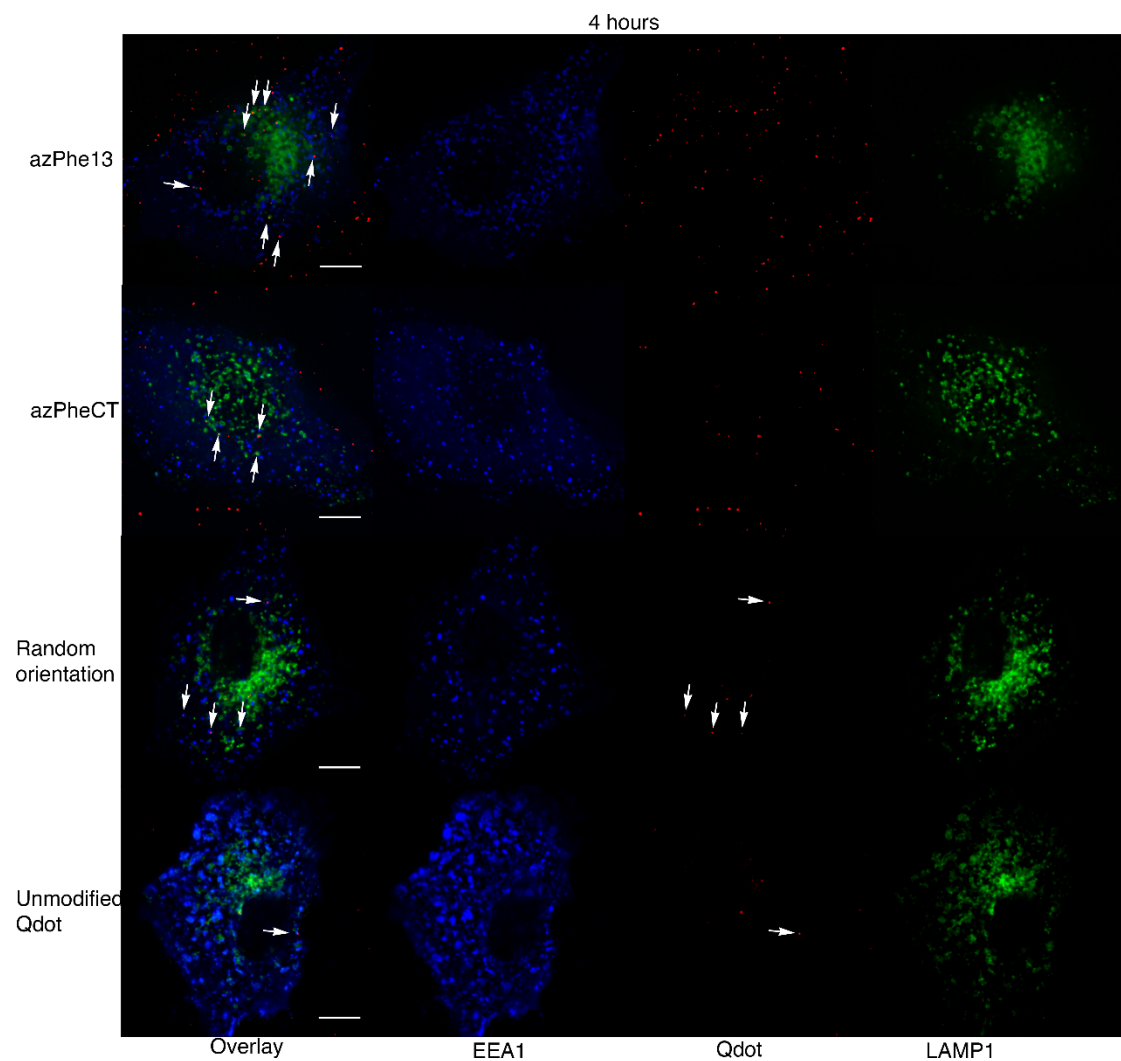
a)

b)

Figure S5. MFI signal of a) monovalent sdAb-Cy5 (40 nM) and b) multivalent sdAb-Qdot (1.5 nM) over 100 seconds as measured from flow cytometry under energy depleting condition. Green – azPhe13 sdAbs, red – azPheCT sdAbs and blue – wild-type/randomly oriented sdAbs.
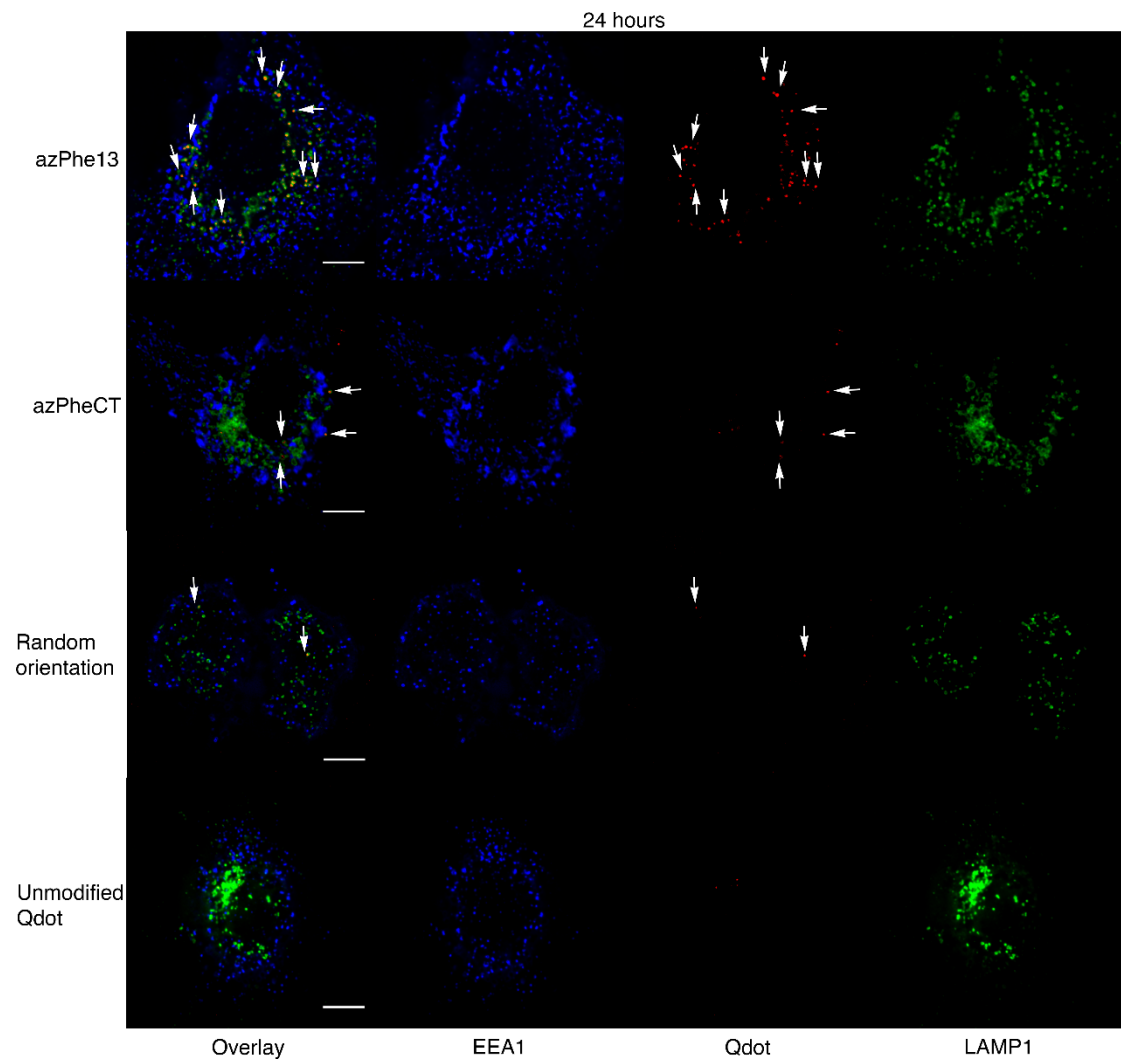
Figure S6. The k_{on} and k_{off} of Cetuximab can be calculated based on linear regression fit determined from k_{obs}. Data are presented as mean ± SEM of n = 3 independent experiments.
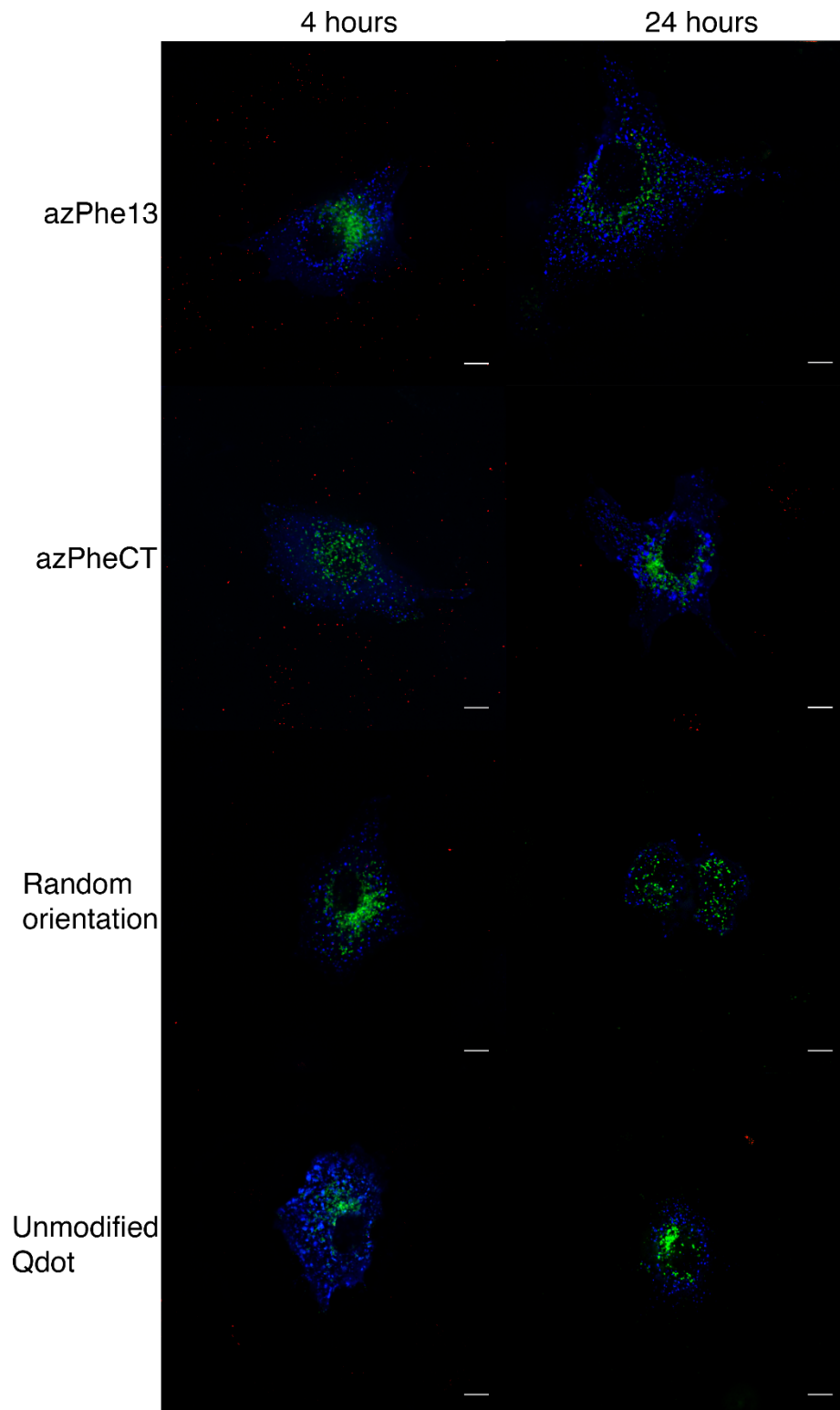

Figure S7. Biotinylated sdAbs with different linker lengths were immobilized onto streptavidin biosensors followed by the addition of free recombinant EGFR to simulate Qdot surface from BLItz. Data are presented as mean ± SD of n = 3 independent experiments. Green – azPhe13 sdAbs, red – azPheCT sdAbs and blue – randomly oriented sdAbs.

Figure S8. Co-localization of azPhe13, azPheCT, randomly oriented sdAb and unmodified Qdot (red) on to GFP-EEA1 (blue) or mApple-LAMP1 (green) transfected A549 cells at 4 hours. Scale bars = 10 μm

Figure S9. Co-localization of azPhe13, azPheCT, randomly oriented sdAb and unmodified Qdot (red) on to GFP-EEA1 (blue) or mApple-LAMP1 (green) transfected A549 cells at 24 hours. Scale bars = 10 μm

Figure S10. Co-localization of azPhe13, azPheCT, randomly oriented sdAb and unmodified Qdot (red) on to GFP-EEA1 (blue) or mApple-LAMP1 (green) transfected A549 cells at 4 and 24 hours. Scale bars = 10 μm

References

(1)   Yong, K. W.; Yuen, D.; Chen, M. Z.; Porter, C. J. H.; Johnston, A. P. R. Pointing in the Right Direction: Controlling the Orientation of Proteins on Nanoparticles Improves Targeting Efficiency. *Nano Lett.* **2019**, *19* (3), 1827–1831.

(2)   Schindelin, J.; Arganda-Carreras, I.; Frise, E.; Kaynig, V.; Longair, M.; Pietzsch, T.; Preibisch, S.; Rueden, C.; Saalfeld, S.; Schmid, B.; Tinevez, J. Y.; White, D. J.; Hartenstein, V.; Eliceiri, K.; Tomancak, P.; Cardona, A. Fiji: An Open-Source Platform for Biological-Image Analysis. *Nat. Methods* **2012**, *9* (7), 676–682.

(3)   Pathak, S.; Davidson, M. C.; Silva, G. A. Characterization of the Functional Binding Properties of Antibody Conjugated Quantum Dots. *Nano Lett.* **2007**, *7* (7), 1839–1845.